5

Experimental Procedure for Rotating Ventilated Disk

Kannan M. Munisamy
Dept. of Mechanical Engineering, College Of Engineering
Universiti Tenaga Nasional, Kajang
Malaysia

1. Introduction

This chapter illustrates experimental procedure and rig development for a ventilated brake disk. Ventilated brake disk is the state of the art technology in automobile braking system. It is well known that the braking capability of brake disk is affected by the rate at which heat is dissipated through forced convection. The rapid increase and decrease of the brake disk temperature could lead to catastrophic failure of the brake disk due to high thermal strains. Heat transfer property enhancement in any ventilated disk design is an important interest to researches. The heat transfer analysis can be conducted experimentally or numerically. Experiment can be carried out on vehicle testing and in laboratory testing procedures. This chapter describes a method for laboratory testing procedure for vehicle disk brake design heat transfer property evaluation.

A rotating test rig is described with unique outflow measurement casing design to restrict outflow with minimum leakage. The casing is important to measure the total air metered through the ventilated disk passage due to inductive air flow. The chapter includes the test procedure and the post processing of the data collected. The devices, such as infrared sensors, thermocouples, flow meter, magnetic speed pick-up and pressure transducers are all connected to Data Acquisition System (DAQ), where the signals are converted to raw data files. The data acquisition module and graphical outputs are shared during the transient recording. The stationary but rotating test rig allows designer to eliminate cross wind effect and other fittings in the car wheel components to focus on the blade geometrical aspect alone. The immobility of the test rig makes it easier to measure the flow pass through and heat transfer from the disk brake.

2. Brake disk experimental rig

A preliminary experimental rig is initially developed to measure the amount of air metered into the ventilated brake disk and the pressure between the rotating blades. The inlet velocity is measured by taking the velocity integral in the inlet ducting using pitot-static tube. Schematic diagrams of the test rig with the components positions shown in picture below. The initial test rig was worth the effort to minimize lead time in designing the rotating test rig with DAQ system and sophisticated measuring equipment.

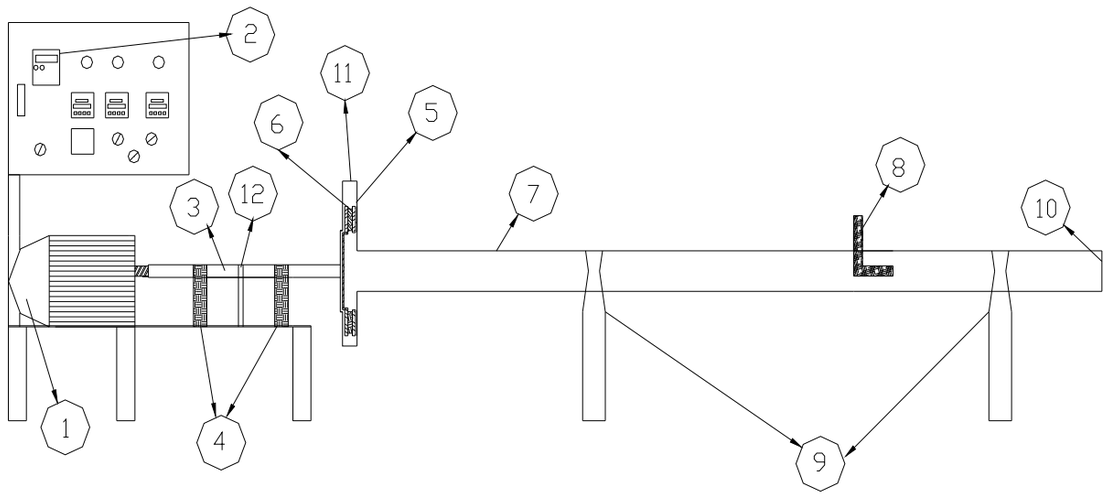

Part No.	Description	Part No.	Description
1	Single Phase Motor	7	Inflow Ducting
2	Motor Speed Controller	8	Pitot-tube Manometer
3	Connecting Shaft	9	Ducting Support
4	Bearing	10	Inflow
5	Disc Brake Casing	11	Outflow
6	Ventilated brake disc specimen	12	Magnetic speed pick-up

Fig. 1. Schematic of Experimental Rig and the Main Components

Test rig shown above used to predict the flow range using pitot tube which is labeled as no. 8. The upgraded version of the experimental rig has ability to measure sophisticated measurements, such as total flow rate, surface temperature and pressure which collected by DAQ. The enhanced version of test rig circuit drawing shown in Fig to observe the position of the measuring device which placed at the test specimen. Moreover the brief explanation of the thermocouple location also has been discussed in Table . There are Pt-type, K-type and infrared type thermocouples involved in the measurements of temperature.

ID	Thermocouple	Location
A	Pt1	R = 125mm
B	Pt2	R = 110mm
C	Pt3	R = 95mm
D	Pt4	R = 125mm
E	Pt5	R = 110mm
F	Pt6	R = 95mm
G	Pt7	Inlet, R = 60mm
H	Pt8	Outlet, R = 130mm
I	K1	Ambient

Table 1. Position of Thermocouple

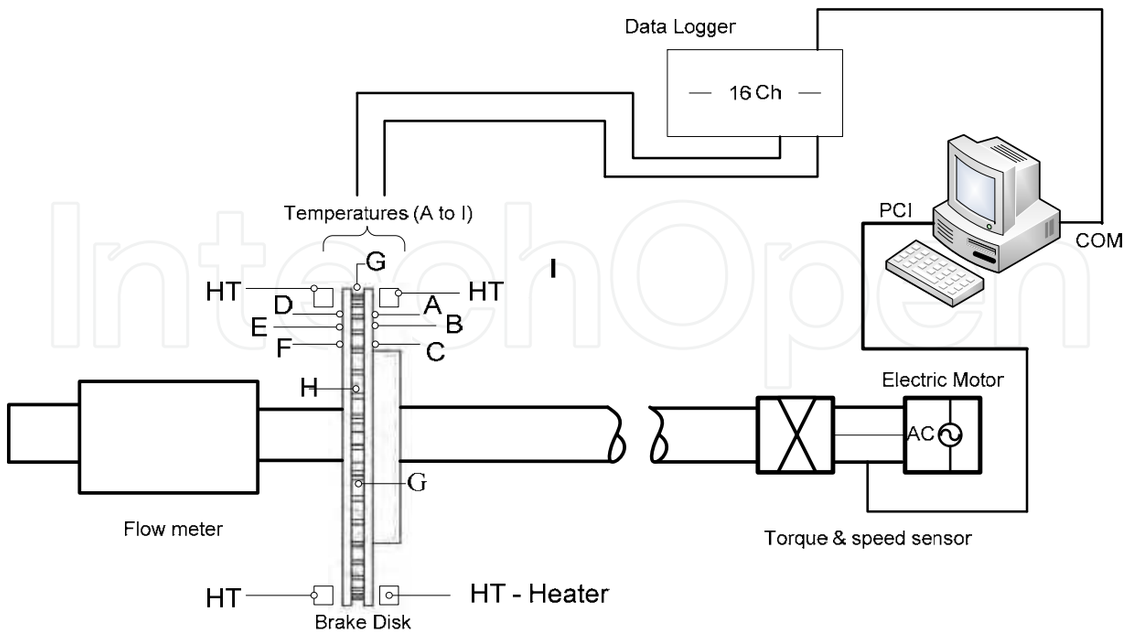

Fig. 2. Ventilated brake disk experimental rig

Fig. illustrates the photographic view of the upgraded experimental rig used. The Fig. show the overall view of the test rig with long intake duct to ensure developed flow at the flow meter. The Figure (a) shows the long air flow ducting to ensure a fully developed flow passes through the flow meter. Figure 3(b) shows the disk brake stationary casing and the manual display of the parameter measurements. The design shows the custom-made Aluminum material casing that guides the outflow radially out and axially directed in through the center of the brake disk with almost zero leakage. The ventilated brake disk of 255mm diameter is fitted with only 1mm clearance between rotating disk and the casing. The tube around the casing is to measure the outlet static pressure.

3. Error analysis

Experiments are basically done to verify some statement, by determining objectives, methodology and research are carried out also at first, followed by progress, results, and analysis with discussion and finally conclusions are made. These are the basic steps on how an experiment is being conducted, and there are no limitations for sub-stages to be included in each step. Specifically, analysis can be categorized to few sub-stages, such as measuring and obtaining some data, tabulate it and plotting a graph based on table. Besides that, error analysis is vital part and it's divided into two fraction; random error and systematic error. These analysis are done mainly to shirk wrong analysis as well provide good accuracy during collecting data from the measurement device.

3.1 Random error

Random errors are errors in measurement that lead to measured values being inconsistent when repeated. The word random indicates that they are inherently unpredictable, and

a)

b)

Fig. 3. Photographs of the upgraded experimental rig

have null expected value, namely, they are scattered about the true value, and tend to have null arithmetic mean when a measurement is repeated several times with the same instrument. Random errors are also can be defined as an error that results from unpredictable variations from one or more influenced quantities. Random error is mainly caused by unpredictable fluctuations in the data of a measurement apparatus, or in the human interpretation of the instrumental reading; these fluctuations may be in part due to interference of the environment with the measurement process. The concept of random error is closely related to the concept of precision. There are no way of perfect experiment to be done without any random error, but the higher the precision of a measurement instrument in an experiment, the smaller the variability (standard deviation) of the fluctuations in the readings.

3.2 Systematic errors

Systematic errors are also known as bias error in measurement which leads to the situation where the mean of many separate measurements differs significantly from the actual value of the measured attribute. Often of several different types of measurement are prone to systematic errors. Sources of systematic error may be imperfect calibration of measurement instruments and sometimes imperfect methods of observation can be either zero error or percentage error.

Systematic errors may also be present in the result of an estimate based on a mathematical model or physical law. For instance, the estimated oscillation frequency of a pendulum will be systematically in error if slight movement of the support is not accounted for. Systematic errors can be either constant, or be related (e.g. proportional or a percentage) to the actual value of the measured quantity, or even to the value of a different quantity.

3.3 Comparison of random errors and systematic errors

Many are still confused between random and systematic errors. Random error will always appear in a measurement and being caused by unpredictable fluctuations in the readings of a measurement apparatus or with experiment conductor's interpretation of the instrumental reading.

On the other side, systematic error is quite predictable, and always either constant or proportional to the true value. It can be eliminated if the cause of the systematic error can be identified. Systematic errors are caused by imperfect calibration of measurement instruments or imperfect methods of observation, and always affect the results of an experiment in a predictable direction. Inversely for random errors, its unpredictable criteria makes the error hardly identified, yet eliminate it. Example, distance measured by radar will be systematically overestimated if the slight slowing down of the waves in air is not accounted for. Incorrect zeroing of an instrument leading to a zero error is an example of systematic error in instrumentation.

4. Measurement devices error analysis

To gather all information regarding systematic errors, user manuals for all equipment were researched. Below is the table describing the channels representing hardware, basic description about the function of the hardware and systematic errors.

CHANNEL	HARDWARE	DESCRIPTION	ERRORS (SYSTEMATIC)
0	Infrared temperature sensor	To measure temperature at outer radius of disc	OS 136 – 1 : 3% of reading or 44°C (8°F) whichever greater. Repeatability: 1% of reading.
1	Infrared temperature sensor	To measure temperature at inner radius of disc	OS 136 – 1 : 3% of reading or 44°C (8°F) whichever greater. Repeatability: 1% of reading.
2	Control panel	Contains controller for tachometer, and power on/off for heater	-
3	-	-	-
4	-	-	-
5	Pt-type temperature sensor	To measure temperature of radiation of disc at top left	Class A : Tolerance ± 0.06% @ 0C Class B : Tolerance ± 0.12 % @ 0C
6	Pt-type temperature sensor	To measure temperature of radiation of disc at top right	Class A : Tolerance ± 0.06% @ 0C Class B : Tolerance ± 0.12 % @ 0C
7	K-type temperature sensor	To measure temperature of air flow through ducting	Linear from 0 °C to +400 °C (3 °C ± 3% of reading)
8	-	-	-
9	Pt-type temperature sensor	To measure temperature of radiation of disc at bottom	Class A : Tolerance ± 0.06% @ 0C Class B : Tolerance ± 0.12 % @ 0C
10	Pressure Tapping / Transducer	To measure pressure change at left inlet of disc	Hysteresis Error 0.5% of FS – Standard Operation, 0.1% of FS High Resolution Mode – Zero Shift.
11	Pressure Tapping / Transducer	To measure pressure change at right inlet of disc	Hysteresis Error 0.5% of FS – Standard Operation, 0.1% of FS High Resolution Mode – Zero Shift.
12	Pressure Tapping / Transducer	To measure pressure change at right outlet of disc	Hysteresis Error 0.5% of FS – Standard Operation, 0.1% of FS High Resolution Mode – Zero Shift.
13	Pressure Tapping / Transducer	To measure ambient pressure	Hysteresis Error 0.5% of FS – Standard Operation, 0.1% of FS High Resolution Mode – Zero Shift.
14	Pressure Tapping / Transducer	To measure pressure change at left outlet of disc	Hysteresis Error 0.5% of FS – Standard Operation, 0.1% of FS High Resolution Mode – Zero Shift.
15	Flow meter	To measure air flow rate through ducting	± 1.5% of measured value (at Qt 100%), ± 5% of measured value (at <Qt*)

Table 2. Table of representative channel, description and systematic error for hardware in Disc Brake Experimental Rig

As in

Table channel 3, 4 and 8 are not connected to any hardware, and might be used in future if more measurement is needed. Similar brand and model is used for each type of sensors, so similar errors are obtained. When calculating for combined errors for certain formulas or equations, the errors for standard operation is chosen. The errors also selected when the variables are in 100% condition, example for flow meter which having two condition of error selection. The first condition of ±1.5% of measured value is chosen because flow rate is 100%, which indicating no disturbance in the flow. For pressure transducer, 0.1% error is chosen in calculation of error analysis, because the Experimental Rig is assumed working under standard operation. Other errors are taken directly, which had given in the respective user manuals that suitable for all kind of condition.

4.1 Pitot-static measurement

The flow measurement is first measured using pitot-static tube. The schematic of the experimental rig illustrated in Fig. . As shown, to constraint the flow through the disk specimen, a custom-made brake disk casing is fabricated. In order to measure the air inflow velocity, an circular duct was built. Additional tapping is also made on the brake disk casing to tap the inlet and outlet pressure between the disk blades in radial direction. This experimental rig can be tested using various brake disk specimen with constant outer diameter. Another constraint to this test rig is the maximum revolution shall go up to 2600 rpm which is equivalent to 320km/h road speed.

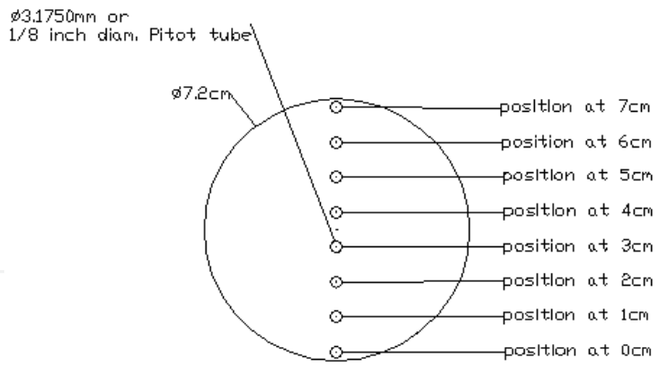

Fig. 4. Traversed Pitot tube positioning at 8 radial points in pipe cross-section

The experimental rig is mainly developed to measure the amount of air metered into the ventilated brake disk and the pressure between the rotating blades. The inlet velocity is measured in the by taking the velocity integral in the inlet ducting. The screen which keeps the flow attached in a ducting is not needed because there is no sudden change in the diameter of the ducting (Mehta, (34)). Then, the entrance length l_e was calculated with reference to Munson et. al. (35)

$$\frac{l_e}{D} = 0.06R_e \tag{1}$$

$$\frac{l_e}{D} = 4.4R_e^{\frac{1}{6}} \quad (2)$$

The equation 1 is for laminar flow and equation 2 is for turbulent flow. The highest Reynolds Number is turbulent. Thus, equation 2 is used to calculate the entrance length. The entrance length l_e of a 2.5m ducting is constructed for the pitot - static tube velocity measurement. Fig shows the pitot - static tube measuring position. The velocity in traverse direction (see Fig is measured using pitot tube with reference to the BS1042. Then, the flow rate is calculated using multiple-application trapezoidal rule. An incline liquid manometer is used to measure the small static pressure difference.

5. Oscillation flow meter (model: DOG)

This device works without any moving parts. An orifice in the lower section generates a flow resistance through which part of the flow is fed into the measuring head. There is then a spontaneous oscillation of the gas in the measuring head. The oscillation frequency is proportional to the flow velocity and consequently to the volume flow. Since the relationship between the flow through the measuring head and the flow through the measuring casing is constant the oscillation frequency also remains directly proportional to the overall volume flow through the device. A hot wire sensor determines the oscillations in the measuring head. A signal transducer feeds the sensor with power supply and amplifies and scales the oscillations. This flow meter manufactured by Kobold. Flow meter's technical information listed as below:-

Measuring accuracy	$\pm$ 1.5% of measuring value at Q_t 100%
Repeatability	0.1% of measured value
Temperature	maximum -20 to 120 ˚C
Materials	
Housing	Stainless Steel 1.4571
Orifice	Stainless Steel 1.4436
Sensing Element	PolyphenyleneSulfida (PPS)
Sensor	Platinum
Gaskets	Silicone

6. Infrared temperature sensor (model OS136 series)

This model is a low cost, super compact infrared transmitter. It measures temperature via non contact, and provides an analog output proportional to the measured temperature. This unit has a fixed Emissivity of 0.95 which makes it easy to measure temperature. The range is larger than the optical field of view of the transmitter. The design, 19mm OD x 89mm length is ideal to measure temperature in confined, and hard to reach places (shown in Fig). This transmitter can operate in an ambient temperature of 0 ˚C to 70 ˚C. There is a warm up period of 2 minute after power up. This flow meter manufactured by Omega Engineering. Its technical information listed as below:-

Measuring Accuracy	3% of Reading
Repeatability	1% of Reading
Temperature	maximum -18 to 204 ˚C
Laser Wavelength	630 – 670 nm
Operating Distance	Up to 9.1 m

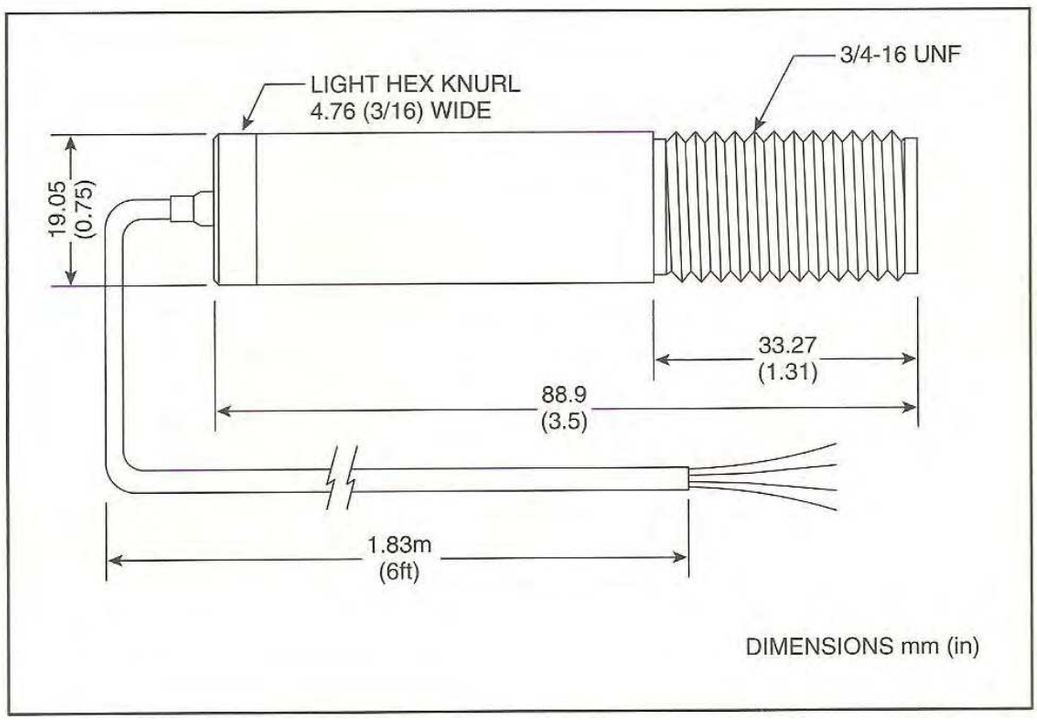

Fig. 5. Infrared Temperature Sensor housing dimension

7. Calculation of convective heat transfer coefficient

The cooling results from test rig were used to determine the convective heat transfer coefficient. The radiation heat transfer was deducted from the disc total heat transfer coefficient and heat conduction to shaft is neglected as the disk brake housing was insulated. At steady state the disk temperature is recorded T_d. The disk temperature will vary in accordance to the convective heat transfer performance of the ventilated blades. The heater is set to be on constant heat flux mode. Thus the heat transfer coefficient is calculated as below:

$$h_c A_W (T_d - T_\infty) = Q_{heater} \tag{3}$$

The equation 3 indicates the heat transfer coefficient, h_c calculated at steady state heating of the brake disk.

8. Error analysis for non-dimensional groups

Error analysis is important to be done for the equations because few variables are involved, which carrying their own errors. So calculation is necessary in order to determine new error

for important equation, which later on used in future application. In this sub-chapter, every detail of calculation, together with its example will be showed. All the calculation below are based on Eq 3.11 & 3.16 of textbook of Experimentation and Uncertainty Analysis for Engineers, 2nd edition, By Hugh W.Coleman and W. Glenn Steele. Pg 51. (Coleman and Steele December 1998)

8.1 Non-dimensional number, Cw

$$\mathrm{Cw} = \frac{Q}{\mu R} \tag{4}$$

Where

Cw: Non-dimensional number
R: Radius of disc brake = 0.1275m
Q: Air flow rate
μ: kinematic viscosity of air = 1.1516E-05 m²/s

$$\frac{U_{Cw}^2}{Cw^2} = \left(\frac{Q}{Cw} \bullet \frac{\partial Cw}{\partial Q}\right)^2 \left(\frac{U_Q}{Q}\right)^2 + \left(\frac{\mu}{Cw} \bullet \frac{\partial Cw}{\partial \mu}\right)^2 \left(\frac{U_\mu}{\mu}\right)^2 + \left(\frac{R}{Cw} \bullet \frac{\partial Cw}{\partial R}\right)^2 \left(\frac{U_R}{R}\right)^2$$

$$\frac{U_{Cw}^2}{Cw^2} = \frac{U_Q^2}{Q^2} + \frac{U_\mu^2}{\mu^2} + \frac{U_R^2}{R^2}$$

μ andR are constant, uncertainties related to these constants are equals to zero, so it can be omitted from the equation

$$\frac{U_{Cw}^2}{Cw^2} = \frac{U_Q^2}{Q^2} = 1.5\%$$

8.2 Reynolds number, Re

$$\mathrm{Re} = \frac{\boldsymbol{V_{rot}\, R^2}}{\boldsymbol{\mu}} \tag{5}$$

Where

Re: Reynolds Number
V_{rot}: rotational speed
R: radius of the disc brake = 0.1275m
μ: kinematic viscosity of air = 1.1516E-05 m²/s

$$\frac{U_{Re}^2}{Re^2} = \left(\frac{V_{rot}}{Re} \bullet \frac{\partial Re}{\partial V_{rot}}\right)^2 \left(\frac{U_{V_{rot}}}{V_{rot}}\right)^2 + (2)^2 \left(\frac{R}{Re} \bullet \frac{\partial Re}{\partial R}\right)^2 \left(\frac{U_R}{R}\right)^2 + \left(\frac{\mu}{Re} \bullet \frac{\partial Re}{\partial \mu}\right)^2 \left(\frac{U_\mu}{\mu}\right)^2$$

$$\frac{U_{Re}^2}{Re^2} = \frac{U_{V_{rot}}^2}{{V_{rot}}^2} + (2)^2 \frac{U_R^2}{R^2} + \frac{U_\mu^2}{\mu^2}$$

Since R, V_{rot} and μ are constant, uncertainties related to these constants are equals to zero, so it can be omitted from the equation

$$\frac{U_{Re}^2}{Re^2} = 0\%$$

8.3 Head rise, Hr

$$\mathrm{Hr} = \frac{\boldsymbol{P_1 - P_\infty}}{\boldsymbol{\rho g}} \tag{6}$$

Where

P_1 - P_∞: Pressure Difference
ρ : density = 1.17 kg/m^3
g : gravity constant = 9.81 m^2/s

$$\frac{U_{Hr}^2}{Hr^2} = \left(\frac{\mathrm{P1-P\infty}}{Hr} \bullet \frac{\partial Hr}{\partial \mathrm{P1-P\infty}}\right)^2 \left(\frac{U_{\mathrm{P1-P\infty}}}{\mathrm{P1-P\infty}}\right)^2 + \left(\frac{\rho}{Hr} \bullet \frac{\partial Hr}{\partial \rho}\right)^2 \left(\frac{U_\rho}{\rho}\right)^2 + \left(\frac{g}{Hr} \bullet \frac{\partial Hr}{\partial g}\right)^2 \left(\frac{U_g}{g}\right)^2$$

$$\frac{U_{Hr}^2}{Hr^2} = \frac{U_{\mathrm{P1-P\infty}}^2}{\mathrm{P1-P\infty}^2} + \frac{U_\rho^2}{\rho^2} + \frac{U_g^2}{g^2}$$

Since ρ and g are constant, uncertainties related to these constants are equals to zero, so it can be omitted from the equation

$$\frac{U_{Hr}^2}{Hr^2} = \frac{U_{\mathrm{P1-P\infty}}^2}{\mathrm{P1-P\infty}^2} = 0.1\%$$

8.4 Pressure rise, Pr

$$\mathrm{Pr} = \frac{\boldsymbol{Hr.\ g}}{\boldsymbol{V_{rot.}^2\ R^2}} \tag{7}$$

Where
Pr: Pressure rise
Hr: Head rise
g: gravity constant = 9.81 m^2/s
Vrot: rotational speed
R: radius of the disc brake = 0.1275m

$$\frac{U_{Pr}^2}{Pr^2} = \left(\frac{\mathrm{Hr}}{Pr} \bullet \frac{\partial Pr}{\partial \mathrm{Hr}}\right)^2 \left(\frac{U_{\mathrm{Hr}}}{\mathrm{Hr}}\right)^2 + \left(\frac{\mathrm{g}}{Pr} \bullet \frac{\partial Pr}{\partial \mathrm{g}}\right)^2 \left(\frac{U_g}{g}\right)^2 + \left(\frac{V_{rot}}{Pr} \bullet \frac{\partial Pr}{\partial V_{rot}}\right)^2 \left(\frac{U_{V_{rot}}}{V_{rot}}\right)^2 + \left(\frac{\mathrm{R}}{Pr} \bullet \frac{\partial Pr}{\partial \mathrm{R}}\right)^2 \left(\frac{U_{\mathrm{R}}}{\mathrm{R}}\right)^2$$

$$\frac{U_{Pr}^2}{Pr^2} = \frac{U_{\mathrm{Hr}}^2}{\mathrm{Hr}^2} + \frac{U_{\mathrm{g}}^2}{\mathrm{g}^2} + \frac{U_{V_{rot}}^2}{{V_{rot}}^2} + \frac{U_{\mathrm{R}}^2}{\mathrm{R}^2}$$

Since g, V_{rot} and R are constant, uncertainties related to these constants are equals to zero, so it can be omitted from the equation

$$\frac{U_{Pr}^2}{Pr^2} = \frac{U_{\mathrm{Hr}}^2}{\mathrm{Hr}^2} = 0.1\%$$

8.5 Nusselt number, Nu

$$\mathrm{Nu} = \frac{\boldsymbol{C1 - C2\ [T_d^4(r) - T_{heater}^4]}}{\boldsymbol{T_d(r) - T\infty}} \tag{8}$$

Where

Nu: Nusselt number
C_1: constant from equation C1 = $\lambda air\left(\frac{\partial T(r)}{\partial x}\right)$

C_2: constant from equation C2 = $\frac{\sigma F \varepsilon_d \varepsilon_H}{1-F^2(1-\varepsilon_d)\varepsilon_H}$

T_d: temperature of disc

T_{heater}: Temperature of heater

T_∞ : Ambient temperature

C1 and C2 are constants obtained from literature review, so uncertainties for these constants are equals to zero and error analysis calculation for these constants are assumed zero

$$\frac{U_{Nu}^2}{Nu^2} = \left(\frac{C1}{Nu} \bullet \frac{\partial Nu}{\partial C1}\right)^2 \left(\frac{U_{C1}}{C1}\right)^2 + \left(\frac{C2}{Nu} \bullet \frac{\partial Nu}{\partial C2}\right)^2 \left(\frac{U_{C2}}{C2}\right)^2 + (4)^2 \left(\frac{Td(r)-Theater}{Nu} \bullet \frac{\partial Nu}{\partial Td(r)-Theater}\right)^2 \left(\frac{U_{Td(r)-Theater}}{Td(r)-Theater}\right)^2 + \left(\frac{Td(r)-T\infty}{Nu} \bullet \frac{\partial Nu}{\partial Td(r)-T\infty}\right)^2 \left(\frac{U_{Td(r)-T\infty}}{Td(r)-T\infty}\right)^2$$

$$\frac{U_{Nu}^2}{Nu^2} = \frac{U_{C1}^2}{C1^2} + \frac{U_{C2}^2}{C2^2} + (4)^2 \frac{U_{Td(r)-Theater}^2}{Td(r)-Theater^2} + \frac{U_{Td(r)-T\infty}^2}{Td(r)-T\infty^2}$$

$\frac{U_{Nu}^2}{Nu^2}$= (16) (0.0006) + (0.0006)

= 0.0096 + 0.0006

= 0.0102

= 1.02%

9. Disk brake experimental rig procedure

The test rig developed with established test procedure. The incorporation of the hardware and the software is described briefly below. Measuring devices such as infrared sensors, flow meter and pressure transducers are all connected to Data Acquisition System (DAQ), which receives reading in raw data. Device Manager and Wavescan 2.0 software's used in this experimental procedure to capture data in real time. The chart in Fig. illustrates the test procedure. The steady state highest temperature value is recorded for the supplied power input at the heater. Then cooling temperature rate can be measured.

Device Manager software used to capture and convert data into spread sheet. The general description of the steps can be found in the flow chart Fig. Firstly, the Device Manager is opened and synchronized. Then all 16 channels are checked to be functioning in good condition as in Fig. The output window with 16 channels turned on can be seen in Fig. After the data capturing is started the window will look like in the Fig. Once the data capturing stopped the data can be converted into spread sheet for further exploitation with the button shown in Fig.

10. Results for a disk brake sample

The experimental rig can be exploited in accordance to the research problem statement by the researcher. The results that were obtained for a study on straight blade ventilated brake disk are shared below. The Figure 12 shows the mass flow rate obtain from the gas flow meter. In this particular study it is even validated against pitot static tube measurement done at multipoint inside the air flow duct. The figure 13 shows the heat transfer coefficient calculated from the experimental analysis is presented against the disk brake rotation speed. The results are checked with numerical data labeled "CFD" for computational fluid dynamics. Following that the no-dimensional parameter Nusselt number if also plotted against rotational Reynolds number. The raw data from the experimental is at the discretion of the researcher to be post-processed in any convenient way for critical analysis.

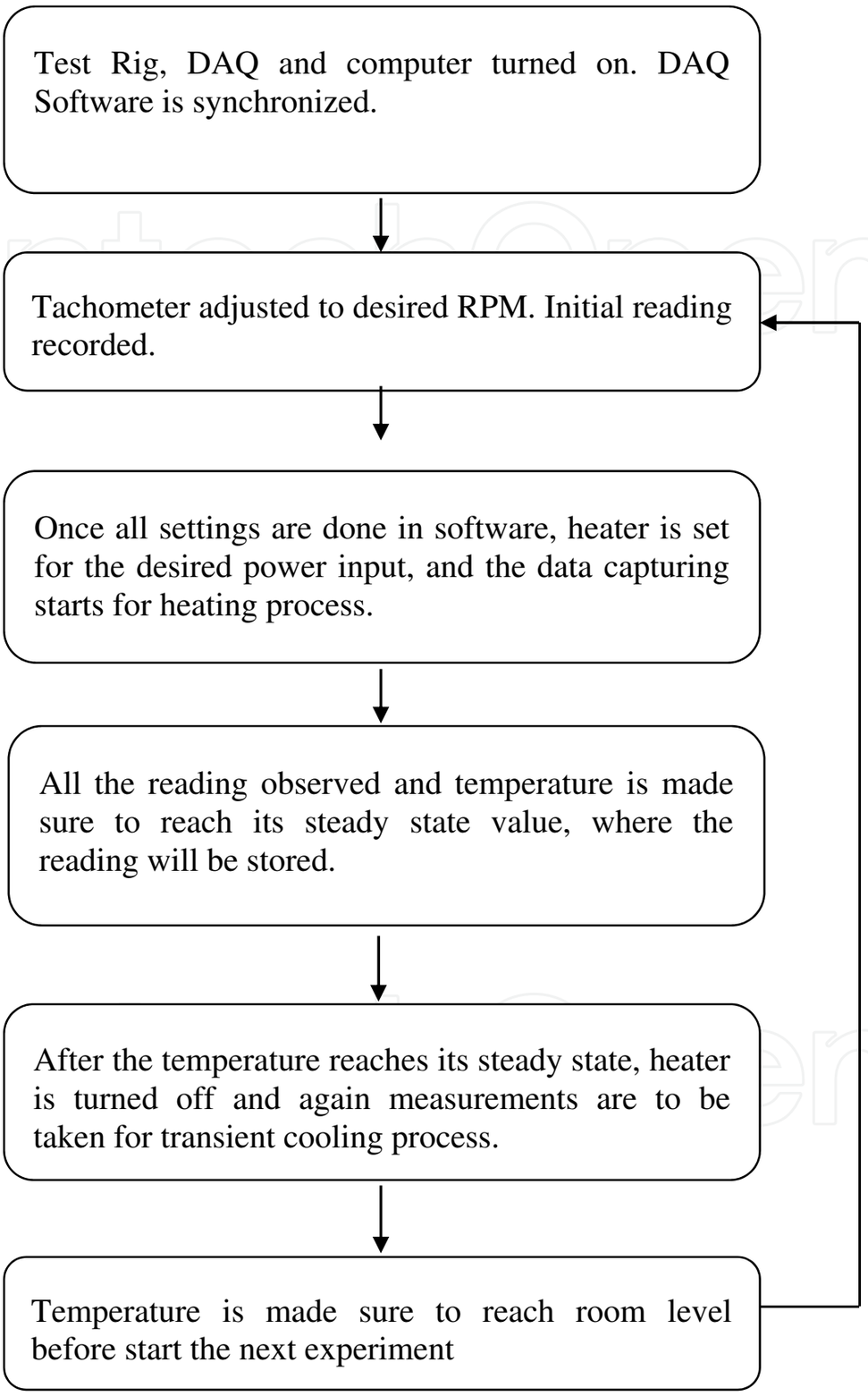

Fig. 6. Flow chart of procedures for Experimental Rig of Disc Brake

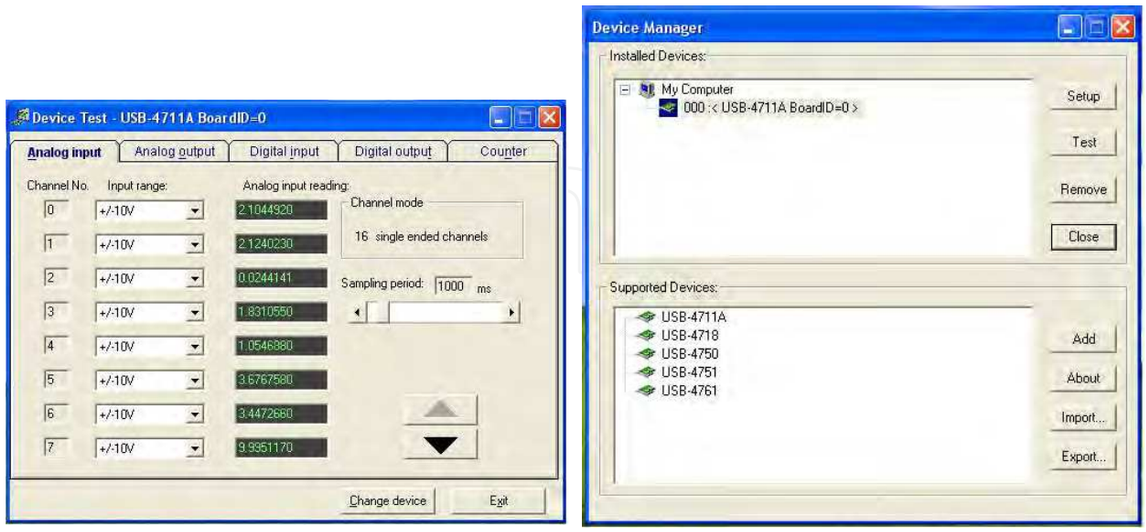

Fig. 7. Device Manager and Device Test

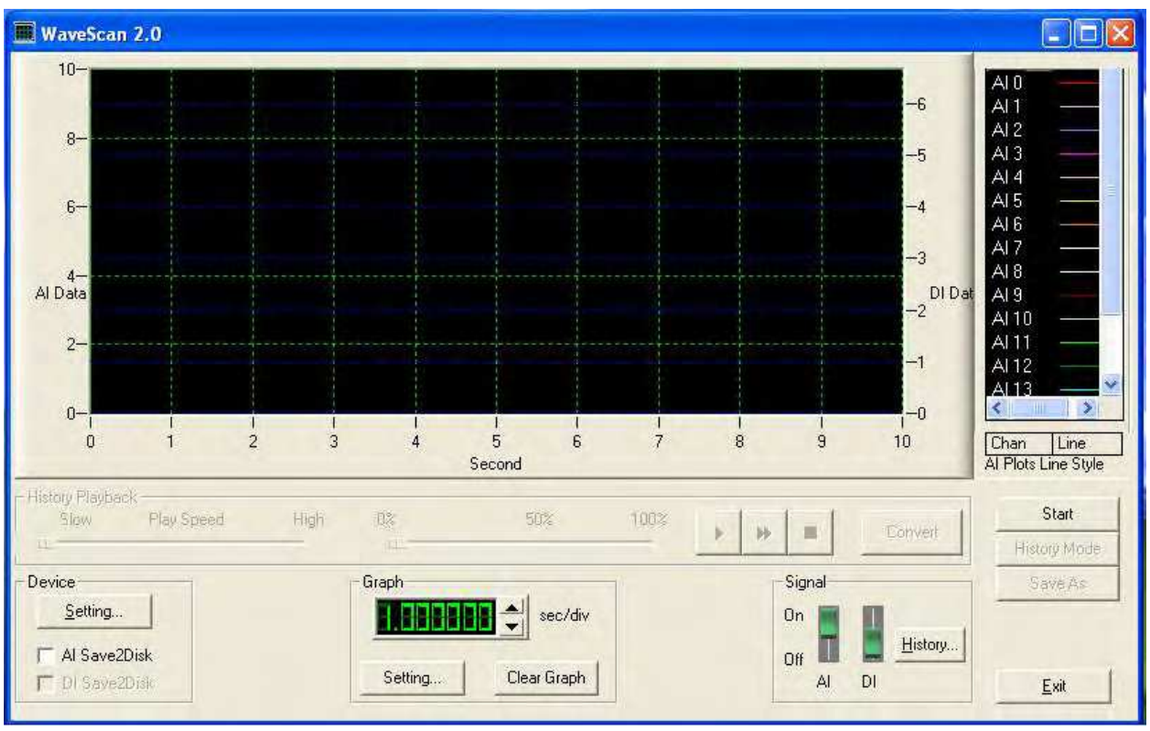

Fig. 8. Analog Signal and channels can be seen on top right side of box

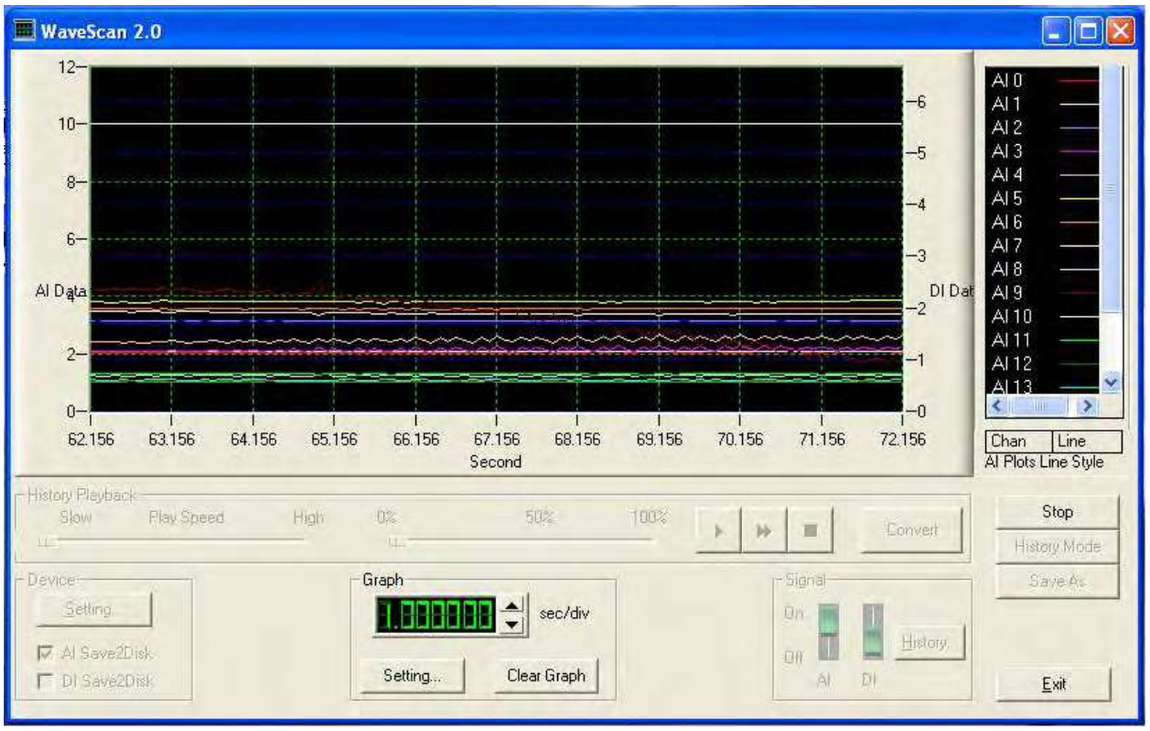

Fig. 9. Raw results with analog signal upon capturing started for all channel

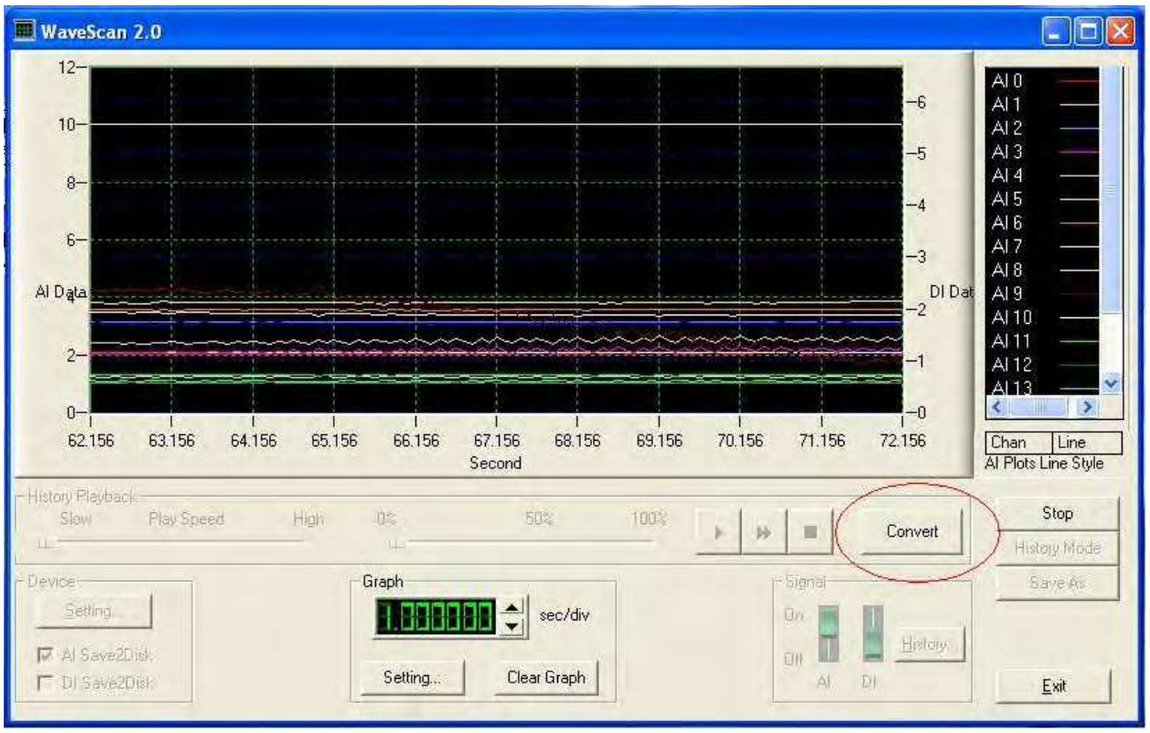

Fig. 10. Wavescan box appeared to convert (in red circle) raw data to spread sheet format

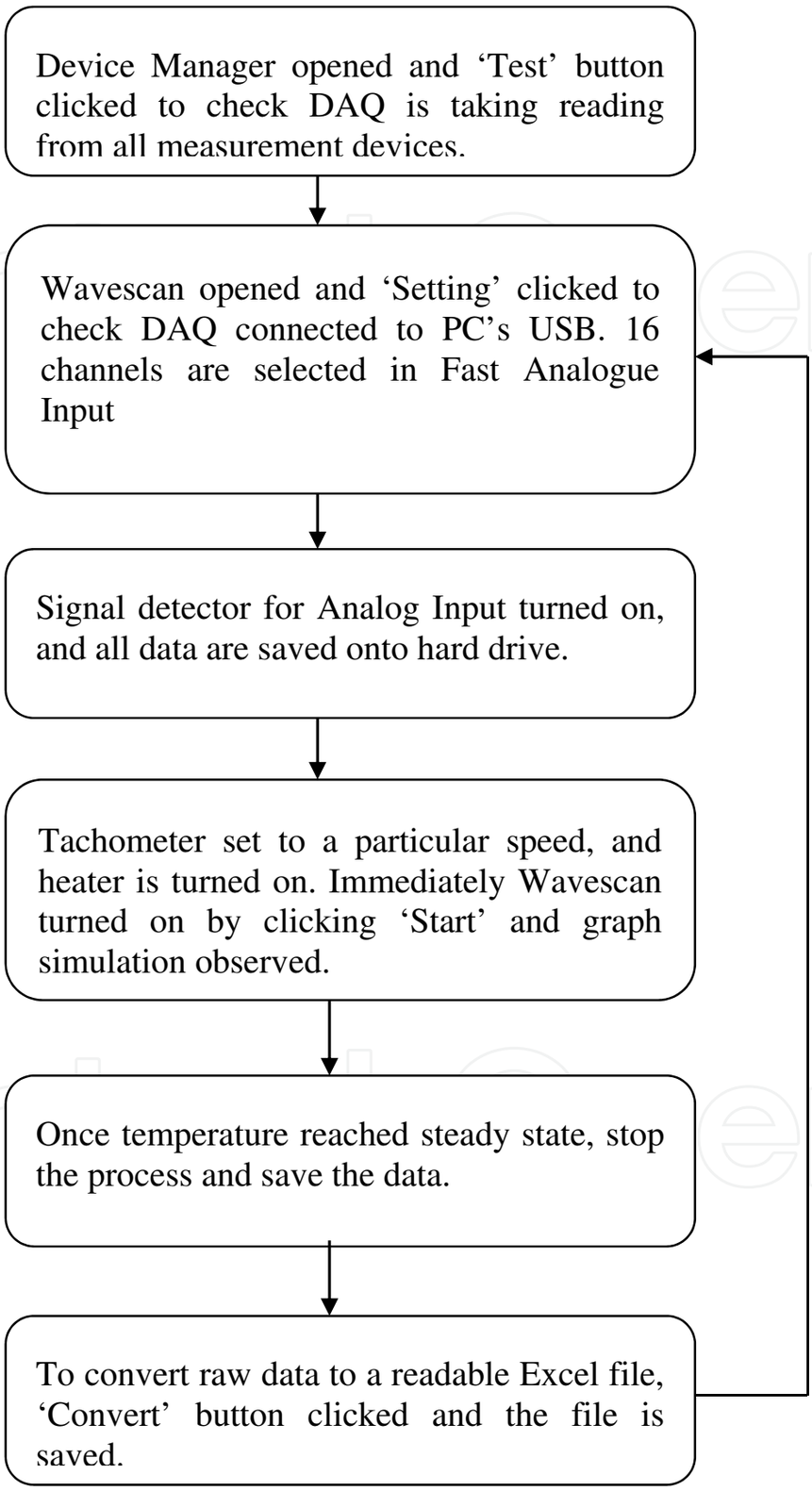

Fig. 11. Flow chart of software evaluation procedures

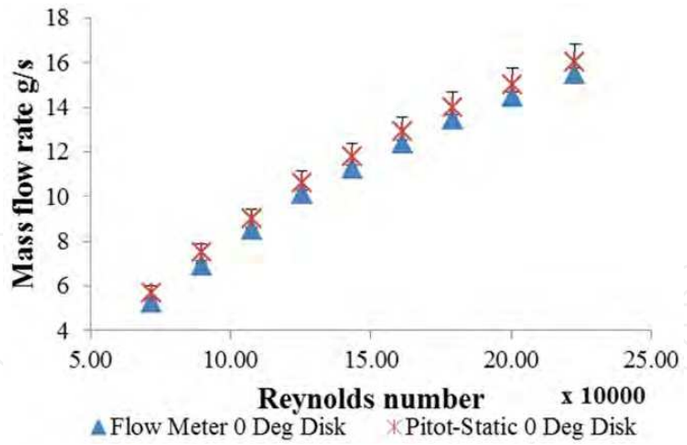

Fig. 12. Mass flow rate measured using flow meter and pitot-static manometer for straight blade brake Disk

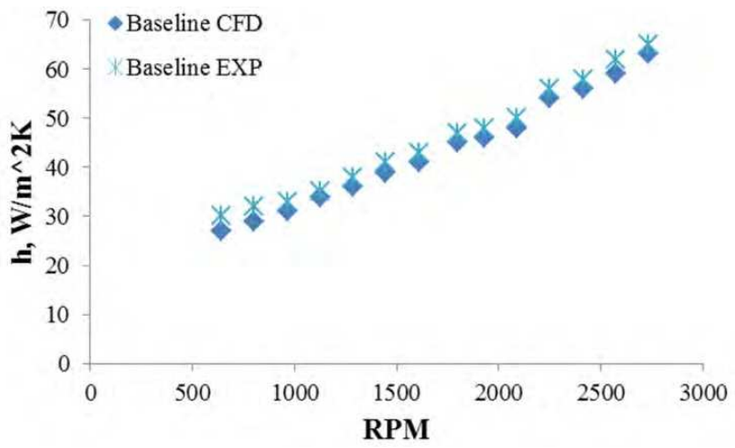

Fig. 13. Validation of CFD modeling with experimental of heat transfer coefficient for baseline brake disk for all rotational speed

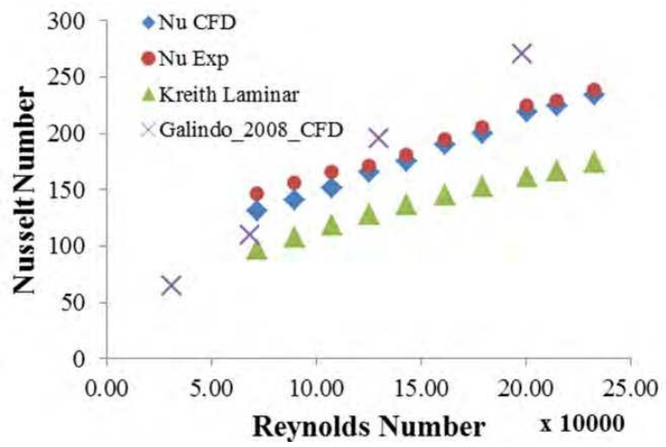

Fig. 14. Validation of CFD modeling with experimental of average Nusselt number for baseline disk brake specimen

11. Conclusion

The experimental rig is a control environment to focus on the heat transfer enhancement of the disk brake alone. The parameters like mass flow rate and Nusselt number is used for classification of the trend of heat transfer characteristics.

For instance for the above Figure 14 nusselt number plot, an expression can be derived with with curve fitting R^2 value less than 1.

For the low speed region where Reynolds number < 2.4 X 10^5 the Nusselt is correlated with Reynolds number with the relationship is given by:

$$Nu = \frac{h_c d_o}{2k} = 0.5 \left(\frac{\omega d_o^2}{4\nu}\right)^{0.50} \tag{9}$$

The Nusselt number against Rotational Reynolds number is given for references.

For the laminar flow condition, the Kreith et. al. (7) correlation is given in equation 10:

$$Nu = \frac{h_c d_o}{2k} = 0.36 \left(\frac{\omega d_o^2}{4\nu}\right)^{0.5} \tag{10}$$

The best fit is given by power of 0.5 for laminar flow condition which agrees well with Kreith (Kreith, Taylor, and Chong, 1959) as in the equation 10.

The experimental procedure described in this chapter can be cost effective to design an improved brake disk for industrial application on vehicles. The rig also demonstrates confident results to be used as significant contribution in disk brake heat transfer area.

12. References

Coleman, Hugh W., and W. Glenn Steele. *Experimentation and Uncertainty Analysis for Engineers.* New York: John Wiley & Sons, December 1998.

Kreith, F., Taylor, J.H., and Chong, Heat and mass transfer from a rotating disk, Journal of Heat Transfer, 1959, ol 81,pp 95-195

Mehta, R. D., and P. Bradshaw. "Technical notes, design rules for small low speed wind tunnels." (The aeronautical journal of the royal aeronautical society) 1979: 443-449.

Munsun, B. R., D. F. Young, and T. H. Okishi. "Fundamentals of fluid mechanics." (John wiley & Sons Inc) 1998.

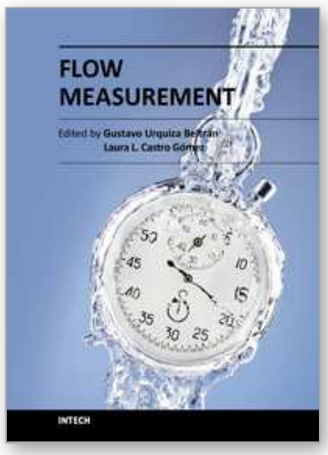

Flow Measurement

Edited by Dr. Gustavo Urquiza

ISBN 978-953-51-0390-5
Hard cover, 184 pages
Publisher InTech
Published online 28, March, 2012
Published in print edition March, 2012

The Flow Measurement book comprises different topics. The book is divided in four sections. The first section deals with the basic theories and application in microflows, including all the difficulties that such phenomenon implies. The second section includes topics related to the measurement of biphasic flows, such as separation of different phases to perform its individual measurement and other experimental methods. The third section deals with the development of various experiments and devices for gas flow, principally air and combustible gases. The last section presents 2 chapters on the theory and methods to perform flow measurements indirectly by means on pressure changes, applied on large and small flows.

How to reference

In order to correctly reference this scholarly work, feel free to copy and paste the following:

Kannan M. Munisamy (2012). Experimental Procedure for Rotating Ventilated Disk, Flow Measurement, Dr. Gustavo Urquiza (Ed.), ISBN: 978-953-51-0390-5, InTech, Available from: http://www.intechopen.com/books/flow-measurement/experimental-procedure-for-rotating-ventilated-disk

INTECH
open science | open minds

InTech Europe
University Campus STeP Ri
Slavka Krautzeka 83/A
51000 Rijeka, Croatia
Phone: +385 (51) 770 447
Fax: +385 (51) 686 166
www.intechopen.com

InTech China
Unit 405, Office Block, Hotel Equatorial Shanghai
No.65, Yan An Road (West), Shanghai, 200040, China
中国上海市延安西路65号上海国际贵都大饭店办公楼405单元
Phone: +86-21-62489820
Fax: +86-21-62489821

IntechOpen